

## Symmetries and mean-field phases of the extended Hubbard model

Anders B. Eriksson,\* Torbjörn Einarsson, and Stellan Östlund

*Institute of Theoretical Physics, Chalmers University of Technology and Gothenburg University, S-41296 Göteborg, Sweden*

(Received 21 November 1994; revised manuscript received 3 March 1995)

The two-dimensional extended Hubbard model that includes a nearest-neighbor Heisenberg interaction is studied using a mean-field theory where quasiparticles are defined by an  $U(8)$  group of canonical transformations permitting both broken gauge, spin, and sublattice symmetry. The theory is further extended to incorporate a possible twist in the spin-quantization axis, so that the competition between superconductivity, charge-density waves, and Néel and spiral antiferromagnetic order can be monitored within one single theory. Our results for positive Hubbard  $U$  and Heisenberg exchange  $J$  suggest that antiferromagnetic ordering dominates close to half-filling, while spiral states and  $d$ -wave superconductivity compete when doping is introduced. For moderate values of  $J$ , we find a phase diagram where a phase transition occurs from an antiferromagnet to a  $d$ -wave superconductor as doping is increased. A narrow region of  $(s + id)$ -wave superconductor is found for some values of  $J$  and  $U$ .

### I. INTRODUCTION

For many years the two-dimensional (2D) Hubbard and “extended” Hubbard model have served as simple models of high- $T_c$  materials and a paradigm of strongly correlated electrons. However, despite many creative attempts to develop approximations to attack the problem, the 2D Hubbard model has defied a definitive analysis.

In contrast to many of those efforts, the goal in the present paper is not to try to model the behavior of high- $T_c$  superconductors or even to make particularly strong statements about the 2D Hubbard model. Rather, we wish to make a definitive analysis of the BCS mean-field theory, an approximation method that has been remarkably successful in gaining information about simpler model systems with both broken spin and gauge symmetry. It is clearly important that we know what this simple approximation has to say about the Hubbard model before we can be confident in applying more sophisticated techniques.

Although the program sounds straightforward, the method becomes surprisingly complicated if one insists on preserving the symmetries known to exist in the Hubbard model at half-filling. The complication is due to the exact  $SO(4) \approx SU(2) \times SU(2)$  symmetry<sup>1</sup> precisely at half-filling and that this symmetry mixes many phases that are typically ignored in simpler calculations. To do a proper job, we must therefore include all the order parameters that have been discussed before for this system, among them spiral spin waves,<sup>2-6</sup> Néel antiferromagnetism,<sup>7-9</sup>  $d$ -wave and  $s$ -wave superconductivity,<sup>7,10-13</sup> as well as all other phases that are related to these via the symmetry group.<sup>14,8</sup>

A consequence is that a multitude of possible order parameters must be retained to provide a self-consistent theory. Our mean-field theory systematically enumerates a very large set of representations of the possible broken symmetries and, among other phases, allows for the possibility of all types of ordered phases that have been

discussed in previous analyses, including antiferromagnetism, spiral spin waves, and  $d$ -wave superconductivity.

The mean-field theory that we employ is based on a  $U(8)$  set of canonical transformations yielding a united treatment of superconductivity,<sup>15-17</sup> charge-density waves, and spin-density waves<sup>18</sup> as was first demonstrated by Solomon and Birman<sup>19</sup> in 1987. The theory is analogous to the use of  $U(2)$  transformations in the analysis of broken gauge symmetry in BCS theory.<sup>15,16</sup>

The organization of the rest of this paper is the following: after providing a brief review of related results in Sec. II, we analyze the symmetry of the Hubbard model in Sec. III. The representations of the  $SU(2) \times SU(2)$  symmetry group is made via an  $8 \times 8$  Clifford algebra, which provides a generalization of the Dirac and Pauli matrices used previously in the Nambu formalism applied in the study of BCS theory and  $^3\text{He}$ .<sup>20</sup> In Sec. IV, we derive the mean-field theory for the Hubbard model at half-filling and introduce the point-group symmetry, while in Sec. V we extend the analysis to include the possibility of spiral antiferromagnetic states that have been proposed as likely phases away from half-filling. We discuss the reformulation of the self-consistent equations in Sec. VI, and the numerical solution procedure in Sec. VII. Our results are presented in the form of phase diagrams in Sec. VIII, before the final discussion in Sec. IX. Appendixes provide additional mathematical details.

### II. BACKGROUND

The Hubbard model is given by the Hamiltonian

$$H = H_0 - \mu \hat{N} + H_{\text{Hubb}}, \quad (1)$$

where

$$H_0 = -t \sum_{\langle \mathbf{R}, \mathbf{R}' \rangle, \sigma} (c_{\mathbf{R}, \sigma}^\dagger c_{\mathbf{R}', \sigma} + \text{H.c.}), \quad (2)$$

$$\hat{N} = \sum_{\mathbf{R},\sigma} n_{\mathbf{R},\sigma}, \quad (3)$$

$$H_{\text{Hubb}} = U \sum_{\mathbf{R}} (n_{\mathbf{R},\uparrow} - \frac{1}{2})(n_{\mathbf{R},\downarrow} - \frac{1}{2}), \quad (4)$$

and where  $n_{\mathbf{R},\sigma} = c_{\mathbf{R},\sigma}^\dagger c_{\mathbf{R},\sigma}$ . The sums in the hopping terms are summed over all *pairs* of nearest neighbors on the 2D square lattice. The form of the Hubbard term is chosen so as to make the Hamiltonian particle-hole symmetric, and the system is half-filled (one electron per site) when the chemical potential  $\mu$  is set to zero.

Several extensions to the Hubbard model have been studied. To have the possibility of mimicking the behavior of higher-order terms which would be present in a more sophisticated weak-coupling expansion,<sup>21</sup> and to physically incorporate the effect of spin-spin interactions, we extend our Hamiltonian by adding the nearest-neighbor Heisenberg interaction  $H_{\text{Heis}}$  given by

$$H_{\text{Heis}} = J \sum_{\langle \mathbf{R}, \mathbf{R}' \rangle} \mathbf{S}_{\mathbf{R}} \cdot \mathbf{S}_{\mathbf{R}'}, \quad (5)$$

where  $\mathbf{S}_{\mathbf{R}} = \frac{1}{2} (c_{\mathbf{R},\uparrow}^\dagger c_{\mathbf{R},\downarrow}^\dagger) \boldsymbol{\sigma} (c_{\mathbf{R},\uparrow} c_{\mathbf{R},\downarrow})^T$  and  $\boldsymbol{\sigma}$  is the vector of Pauli matrices. The Heisenberg term breaks neither spin nor pseudospin symmetry, and thus fulfills the most important constraints on effective higher-order terms in a theory for the pure Hubbard model at half-filling.

In principle, we should also investigate the nearest-neighbor Coulomb interaction. Although it may be physically important, it violates pseudospin symmetry which is already broken by the chemical potential term. Since it adds nothing theoretically fundamental to the model, we chose to not include it in our analysis. Another term that we do not include, but nevertheless is interesting since some rigorous results have been obtained,<sup>22–25</sup> is the correlated hopping term

$$X \sum_{\langle \mathbf{R}, \mathbf{R}' \rangle, \sigma} (c_{\mathbf{R},\sigma}^\dagger c_{\mathbf{R}',\sigma} + c_{\mathbf{R}',\sigma}^\dagger c_{\mathbf{R},\sigma}) (n_{\mathbf{R}',-\sigma} + n_{\mathbf{R},-\sigma}). \quad (6)$$

An appropriate starting point is the pure Hubbard model at half-filling. Here, the model is symmetric under the  $SU(2) \times SU(2)$  group of global spin and “pseudospin” rotations,<sup>1,26–31</sup> and the phase diagram is rather well understood.

For positive values of  $U$ , the ground state is expected to be a 2D antiferromagnetic (AF)  $(\pi, \pi)$ , or Néel, state. For large  $U/t$ , second-order perturbation theory in  $t/U$  yields an effective theory equivalent to the spin- $\frac{1}{2}$  Heisenberg antiferromagnet. The order parameter is given by the staggered magnetization, which is a vector which breaks the global  $SU(2)$  spin and the discrete translational symmetry of the underlying model.

For negative  $U$ , the ground state is either an  $s$ -wave superconductor (SC) or a  $(\pi, \pi)$  charge-density wave (CDW). The real and complex part of the SC order parameter together with the CDW order parameter form a triplet which transforms as a vector under  $SU(2)$  pseudospin rotations. The ground state we call “mixed” SC-CDW since each of these phases are degenerate and re-

lated to each other by a continuous symmetry.

The cases of positive and negative  $U$  are directly related via the “Shiba” transformation  $Z$ .<sup>32</sup> This discrete transformation has the effect of changing the sign of  $U$  in the Hubbard model, and also mapping rotations in spin space into rotations in pseudospin space and vice versa. Furthermore, a state with broken pseudospin symmetry for  $U < 0$  (SC or CDW state), has a direct mapping to a state with broken spin symmetry (an AF state), and since SC already appears for an infinitesimal negative value of  $U$ , AF order must appear for an infinitesimal positive value. Hence there is no Mott transition as a function of  $U/t$ , and the Néel order persists for all positive values of  $U$ .

Away from half-filling, we are less certain of what phases may occur. The pseudospin symmetry is broken, with only the  $U(1)$  gauge subgroup remaining. Spiral spin waves, where the antiferromagnetic order parameter twists with a pitch along a symmetry axis, has been suggested as a likely candidate. This phase has been seen in several theoretical calculations and has been suggested to explain the incommensurate spin correlations seen experimentally.<sup>2–6</sup> We study this class of states by imposing a twisted spin quantization axis in the generalized Hubbard Hamiltonian *before* it is analyzed by the Hartree-Fock-Bogoliubov method.<sup>4</sup>

### III. GROUP-THEORETICAL FRAMEWORK

Our employment of the  $U(8)$  symmetry is, in principle, close to the one by Solomon and Birman.<sup>19</sup> However, since we here study an explicit model, we need to specify our basis and its relation to the order parameters, and in order to facilitate for the reader to understand our results we discuss in the following our approach in some detail.

#### A. Using multispinors to represent symmetries of the Hubbard model

Let us first consider the noninteracting theory  $H = H_0$  at  $\mu = 0$  defined for a square system with  $N$  sites, periodic boundary conditions, and lattice constant 1. This is simply diagonalized as  $H_0 = \sum_{\mathbf{k}} \epsilon_{\mathbf{k}} c_{\mathbf{k},\sigma}^\dagger c_{\mathbf{k},\sigma}$ , where the  $\mathbf{k}$  sum runs over  $N$  points in the first Brillouin zone (BZ). The single-particle dispersion relation is  $\epsilon_{\mathbf{k}} = -2t(\cos k_x + \cos k_y)$ . To make manifest the particle-hole symmetry, we define the vector  $\mathbf{Q} = (\pi, \pi)$  and the operators

$$\begin{aligned} a_{\mathbf{k},\sigma}^\dagger &\equiv c_{\mathbf{k},\sigma}^\dagger, & \text{when } \epsilon_{\mathbf{k}} < 0, \\ b_{\mathbf{k},\sigma}^\dagger &\equiv c_{\mathbf{k}+\mathbf{Q},\sigma}^\dagger, & \text{when } \epsilon_{\mathbf{k}+\mathbf{Q}} > 0. \end{aligned} \quad (7)$$

In terms of these operators,  $H_0$  is written as

$$\begin{aligned} H_0 = \sum_{\mathbf{k},\sigma}'' \epsilon_{\mathbf{k}} (a_{\mathbf{k},\sigma}^\dagger a_{\mathbf{k},\sigma} - b_{\mathbf{k},\sigma}^\dagger b_{\mathbf{k},\sigma} \\ - a_{-\mathbf{k},\sigma} a_{-\mathbf{k},\sigma}^\dagger + b_{-\mathbf{k},\sigma} b_{-\mathbf{k},\sigma}^\dagger), \end{aligned} \quad (8)$$

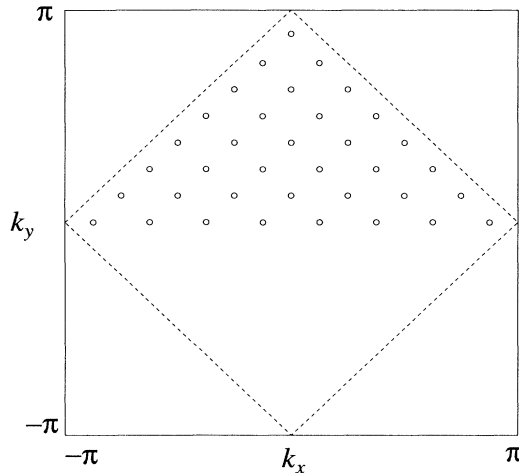


FIG. 1. The first Brillouin zone of the square lattice with lattice constant 1. The line  $\epsilon_{\mathbf{k}} = 0$  is indicated as well as the  $\mathbf{k}$  points in the reduced zone that are used in a numerical simulation with 32  $\mathbf{k}$  points (Sec. VII). The contributions from the points on the  $k_x$  axes are scaled down by a factor of 2 since they would otherwise be overcounted.

where the summation denoted by  $\sum''$  runs over the four times reduced Brillouin zone corresponding to  $\epsilon_{\mathbf{k}} < 0$  and  $k_y \geq 0$  (see Fig. 1). Note the special order of the operators in Eq. (8).

We next introduce the “Shiba” transformation  $Z$  which acts on the *position space* creation and destruction operators  $c_{\mathbf{r},\sigma}^\dagger$  through the canonical transformation  $c_{\mathbf{r},\downarrow}^\dagger \mapsto (-1)^{\mathbf{r}} c_{\mathbf{r},\downarrow}^\dagger$ ,  $c_{\mathbf{r},\uparrow}^\dagger \mapsto c_{\mathbf{r},\uparrow}^\dagger$ , where the factor  $(-1)^{\mathbf{r}} \equiv e^{i\mathbf{Q}\cdot\mathbf{r}}$  induces a change of sign on one sublattice. The Shiba transformation is hence a particle-hole transformation, together with a local change of gauge, which only acts on the spin-down operators.

In reciprocal space, spin rotations and  $Z$  act naturally on the eight-component multispinor  $\Psi_{\mathbf{k}} \equiv (a_{\mathbf{k},\uparrow}, a_{\mathbf{k},\downarrow}, b_{\mathbf{k},\uparrow}, b_{\mathbf{k},\downarrow}, a_{-\mathbf{k},\uparrow}^\dagger, a_{-\mathbf{k},\downarrow}^\dagger, b_{-\mathbf{k},\uparrow}^\dagger, b_{-\mathbf{k},\downarrow}^\dagger)$  which carries definite momentum  $\mathbf{k} \bmod \mathbf{Q}$ . In this basis,  $Z$  is represented by an idempotent matrix whose entries are all zero except  $Z_{1,1} = Z_{3,3} = Z_{5,5} = Z_{7,7} = Z_{2,8} = Z_{4,6} = Z_{6,4} = Z_{8,2} = 1$ , and which acts on  $\Psi_{\mathbf{k}}$  by matrix-vector multiplication,  $\Psi_{\mathbf{k}} \mapsto \Psi_{\mathbf{k}} Z$ . It is well known that  $Z$  is an exact symmetry of  $H_0$  but changes the sign of the Hubbard term  $U$ .<sup>29,31–34</sup> It is also simple to verify that the nearest-neighbor Heisenberg term  $H_{\text{Heis}}$  is invariant under  $Z$ .

A pseudospin transformation  $R'$  is defined as  $R' = ZRZ$  where  $R$  is an ordinary global  $SU(2)$  spin rotation. Since  $[H, Z] = 0$  and  $[H, R] = 0$ , we have  $[H, R'] = 0$ , and since  $Z$  does not commute with  $R$ , we see that the entire symmetry group of  $H$  is  $\mathcal{S} = SU(2) \times SU(2)$ . It follows further that because  $\Psi_{\mathbf{k}}$  defines a representation of both  $R$  and  $Z$ , it also determines a representation of  $\mathcal{S}$ .

## B. A basis spanning the space of Hermitian $8 \times 8$ matrices

To represent the action of spin and pseudospin transformations on the basis  $\Psi_{\mathbf{k}}$ , we introduce a set of seven Hermitian  $8 \times 8$  matrices  $\beta_A$  constructed in blocks from the ordinary Dirac matrices  $\gamma_\nu$  as shown in Table I. By explicit computation, it can be verified that  $\beta_A$  form a Clifford algebra,<sup>35</sup> i.e.,  $\beta_A \beta_B + \beta_B \beta_A = 2g_{AB}$ , where  $g_{AB} = 0$  except for  $g_{00} = \mathbf{1}$  and  $g_{nn} = -\mathbf{1}$ ,  $n = 1, \dots, 6$ .

The  $\beta_A$  matrices have been constructed so that  $(\beta_1, \beta_2, \beta_3)$  transform as a vector under spin rotations and  $(\beta_4, \beta_5, \beta_6)$  transform as a vector under pseudospin rotations, while  $(\beta_4, \beta_5, \beta_6)$  and  $(\beta_1, \beta_2, \beta_3)$  transform as a scalar under spin and pseudospin rotations, respectively. Taking multiple products of the matrices  $\beta_A$ , one can construct a complete basis for the vector space of  $8 \times 8$  Hermitian matrices (with real-valued coefficients). The Clifford algebra contains four independent spin/pseudospin scalars, and it follows that there are also four independent sets of spin and pseudospin vectors and spin $\otimes$ pseudospin tensors, making a total of  $4 \times (1 + 3 + 3 + 9) = 64$  basis elements which together span the space of  $8 \times 8$  Hermitian matrices.<sup>30</sup>

Our goal is to construct a basis that has simple transformation properties under spin and pseudospin rotations, and with the above classification scheme in mind, we label the 64 base matrices by  $B_{\mu\nu}^\kappa$ , where  $0 \leq \mu, \nu, \kappa \leq 3$ . The upper index  $\kappa$  enumerates each of the four independent sets of matrices associated with each of the four scalars. Transformation properties under spin rotations are indexed by  $\mu$ , where scalars carry the index  $\mu = 0$ , while  $\mu = 1, 2, 3$  represents the components of a spin vector. Similarly  $\nu$  identifies pseudospin scalars and vectors. For example,  $B_{01}^2$  transforms as a scalar under spin rotations and as the first component of a pseudospin vector. The matrices  $B_{\mu\nu}^\kappa$  are constructed so that they are not only Hermitian, but also have natural transformation properties under parity, sublattice exchange, and time reversal, and so that the indices  $\mu$  and  $\nu$  are simply interchanged under  $Z$ .

To explicitly construct the basis matrices we introduce the four scalars. Three of them are the identity matrix  $\mathbf{1}$ ,  $\beta_0$ , and  $\Gamma = i\beta_0\beta_1\beta_2\beta_3 = \begin{pmatrix} \gamma_5 & 0 \\ 0 & \gamma_5 \end{pmatrix}$ , where  $\gamma_5$  indicates the

TABLE I. Construction of the  $8 \times 8$   $\beta_A$  matrices from the  $4 \times 4$  Dirac matrices expressed in terms of Pauli matrices. The index  $j$  runs from 1 to 3. The notation  $\gamma_j^*$  denotes complex conjugate (not adjoint).

Pauli	$(\sigma_1, \sigma_2, \sigma_3) = \left[ \begin{pmatrix} 0 & 1 \\ 1 & 0 \end{pmatrix}, \begin{pmatrix} 0 & -i \\ i & 0 \end{pmatrix}, \begin{pmatrix} 1 & 0 \\ 0 & -1 \end{pmatrix} \right]$
$4 \times 4$ Dirac	$\gamma_0 = \begin{pmatrix} \mathbf{1} & 0 \\ 0 & -\mathbf{1} \end{pmatrix} \quad \gamma_j = \begin{pmatrix} 0 & \sigma_j \\ -\sigma_j & 0 \end{pmatrix}$
$8 \times 8$ $\beta_A$	$\beta_0 = \begin{pmatrix} \gamma_0 & 0 \\ 0 & -\gamma_0 \end{pmatrix} \quad \beta_j = \begin{pmatrix} \gamma_j & 0 \\ 0 & \gamma_j^* \end{pmatrix}$
	$\beta_{j+3} = iZ\beta_0\beta_jZ$

pseudoscalar Dirac gamma matrix  $\gamma_5 = i\gamma_0\gamma_1\gamma_2\gamma_3$ ; the fourth scalar matrix is defined as the product  $\beta_0\Gamma$ . The four scalars are denoted  $\Upsilon_\kappa$  with the following identifications:  $\Upsilon_0 = -\mathbf{1}$ ,  $\Upsilon_1 = \beta_0$ ,  $\Upsilon_2 = -\Gamma$ , and  $\Upsilon_3 = -i\Gamma\beta_0$ . To make subsequent formulas simple we also define  $\Omega_0 = \hat{\Omega}_0 = \mathbf{1}$ ,  $\Omega_j = \beta_j$ , and  $\hat{\Omega}_j = \beta_{j+3}$ , where  $j = 1, 2, 3$ . Finally, introducing  $\tau_0 = 1$  and  $\tau_j = \sqrt{-1}$ , the basis matrices are defined by

$$\begin{aligned} B_{\mu,\nu}^\kappa &= \Upsilon_\kappa \Omega_\mu \hat{\Omega}_\nu, & \text{for } \kappa = 0 \text{ or } 1, \\ B_{\mu,\nu}^\kappa &= \tau_\mu \tau_\nu \Upsilon_\kappa \Omega_\mu \hat{\Omega}_\nu, & \text{for } \kappa = 2 \text{ or } 3, \end{aligned} \quad (9)$$

where  $0 \leq \mu, \nu \leq 3$ . The phase factors  $\tau_\mu$  are chosen so as to make  $B_{\mu\nu}^\kappa$  Hermitian.

Letting the subscript  $m$  denote the collection of indices  $\kappa, \mu, \nu$ , we find that the matrices  $B_m$  are orthonormal in the sense that

$$\text{Tr}(B_m B_{m'}) = 8\delta_{m,m'}, \quad (10a)$$

$$B_m B_m = \mathbf{1}. \quad (10b)$$

It follows that an arbitrary Hermitian  $8 \times 8$  matrix  $M$  can be expanded as

$$M = \sum_m \alpha^m B_m, \quad (11)$$

where

$$\alpha^m = \frac{1}{8} \text{Tr}(B_m M). \quad (12)$$

#### IV. WRITING THE MEAN-FIELD HAMILTONIAN IN TERMS OF $8 \times 8$ MATRICES

The interacting Hamiltonian contains not only one-particle but also two-particle terms. We use Wick's factorization<sup>36</sup> to express the expectation values of the two-particle terms as sums of all products of one-particle terms:

$$\begin{aligned} \langle O_1 O_2 O_3 O_4 \rangle &= \langle O_1 O_2 \rangle \langle O_3 O_4 \rangle + \langle O_1 O_4 \rangle \langle O_2 O_3 \rangle \\ &\quad - \langle O_1 O_3 \rangle \langle O_2 O_4 \rangle, \end{aligned} \quad (13)$$

where  $O_i$  denotes any creation or destruction operator. This expansion in pairs of operators forms the basis for the standard BCS-like mean-field theory, which has also been referred to as bosonic linearization.<sup>37</sup>

After transforming  $H + H_{\text{Heis}}$  in Eqs. (1) and (5) to reciprocal space and then applying the factorization we find

$$\begin{aligned} \langle H \rangle &= \sum_{\mathbf{k}, \sigma} (\epsilon_{\mathbf{k}} - \mu) \langle c_{\mathbf{k}, \sigma}^\dagger c_{\mathbf{k}, \sigma} \rangle + \frac{1}{N} \sum_{\substack{\mathbf{k}_1, \mathbf{k}_2, \mathbf{k}_3, \mathbf{k}_4 \\ \sigma, \sigma'}} \delta(\mathbf{k}_1 - \mathbf{k}_2 + \mathbf{k}_3 - \mathbf{k}_4) \left( U \delta_{\sigma, \uparrow} \delta_{\sigma', \downarrow} - \frac{J}{4} (2\gamma_{\mathbf{k}_1 - \mathbf{k}_4} + \gamma_{\mathbf{k}_1 - \mathbf{k}_2}) \right) \\ &\quad \times \left( \langle c_{\mathbf{k}_1, \sigma}^\dagger c_{\mathbf{k}_2, \sigma} \rangle \langle c_{\mathbf{k}_3, \sigma'}^\dagger c_{\mathbf{k}_4, \sigma'} \rangle + \langle c_{\mathbf{k}_1, \sigma}^\dagger c_{\mathbf{k}_4, \sigma'} \rangle \langle c_{\mathbf{k}_2, \sigma} c_{\mathbf{k}_3, \sigma'}^\dagger \rangle - \langle c_{\mathbf{k}_1, \sigma}^\dagger c_{\mathbf{k}_3, \sigma'}^\dagger \rangle \langle c_{\mathbf{k}_2, \sigma} c_{\mathbf{k}_4, \sigma'} \rangle \right), \end{aligned} \quad (14)$$

where  $N$  is the number of lattice sites,  $\gamma_{\mathbf{k}} = \cos(k_x) + \cos(k_y)$ , and  $\delta$  indicate a  $\delta$ -function modulo the reciprocal lattice.

Let us now consider the one-particle expectation values. In ordinary mean-field analysis, all one-particle expectation values that carry nonzero momentum are assumed to be zero. Similarly, in our formalism the natural set of expectation values are related to the elements of the  $8 \times 8$  matrix of operators

$$(\Psi_{\mathbf{k}}^\dagger \otimes \Psi_{\mathbf{k}}) \equiv \begin{pmatrix} a_{\mathbf{k}, \uparrow}^\dagger a_{\mathbf{k}, \uparrow} & a_{\mathbf{k}, \uparrow}^\dagger a_{\mathbf{k}, \downarrow} & \cdots \\ a_{\mathbf{k}, \downarrow}^\dagger a_{\mathbf{k}, \uparrow} & \ddots & \\ \vdots & & \end{pmatrix}, \quad (15)$$

whose expectation values are all of the form  $\langle c_{\mathbf{k}_1, \sigma_1}^\dagger c_{\mathbf{k}_2, \sigma_2} \rangle$ ,  $\langle c_{\mathbf{k}_1, \sigma_1}^\dagger c_{-\mathbf{k}_2, \sigma_2}^\dagger \rangle$ , and  $\langle c_{\mathbf{k}_1, \sigma_1} c_{-\mathbf{k}_2, \sigma_2} \rangle$ , where  $\mathbf{k}_1 = \mathbf{k}_2$  or  $\mathbf{k}_1 - \mathbf{k}_2 = \pm \mathbf{Q}$  with  $\mathbf{Q} = (\pi, \pi)$ . Thus we allow all possible expectation values of operators that carry momentum  $(0, 0)$  or  $(\pi, \pi)$ , and those that carry spin and/or charge to be nonzero. Expectation values carrying momentum  $(\pi, \pi)$  correspond to staggered order, net charge represent superconductors, and net spin is associated with broken spin symmetry.

To make clear the relation between the 64 individual

operators in  $(\Psi_{\mathbf{k}}^\dagger \otimes \Psi_{\mathbf{k}})$  and the irreducible representations (irreps) of  $\text{SU}(2) \times \text{SU}(2)$  we define a set of 64 operators by the following linear combinations:

$$\alpha_{\mathbf{k}}^m = \frac{1}{8} \text{Tr}[B_m (\Psi_{\mathbf{k}}^\dagger \otimes \Psi_{\mathbf{k}})]. \quad (16)$$

We then use these operators to rewrite our mean-field Hamiltonian.

We begin by rewriting the quadratic (one-particle) part of the Hamiltonian in matrix form. From Eq. (8) it is easily seen that  $H_0 = \sum_{\mathbf{k}} \epsilon_{\mathbf{k}} \text{Tr}[B_{00}^1 (\Psi_{\mathbf{k}}^\dagger \otimes \Psi_{\mathbf{k}})] = 8 \sum_{\mathbf{k}} \epsilon_{\mathbf{k}} (\alpha_{00}^1)_{\mathbf{k}}$ , where the basis matrix  $B_{00}^1$  is diagonal and has diagonal elements  $(1, 1, -1, -1, -1, -1, 1, 1)$ . The expectation value of the entire quadratic part of the Hamiltonian then becomes

$$\langle H_0 - \mu \hat{N} \rangle = 8 \sum_{\mathbf{k}} \epsilon_{\mathbf{k}} \left( \underbrace{\langle (\alpha_{00}^1)_{\mathbf{k}} \rangle}_{\text{hop}} - \mu \underbrace{\langle (\alpha_{03}^1)_{\mathbf{k}} \rangle}_{\text{fill}} \right). \quad (17)$$

The interaction (two-particle) part of  $\langle H \rangle$  may be evaluated in a similar manner. To simplify the corresponding expression, we introduce some shorthand notation. Let  $\langle \alpha_{\mu\nu}^{\kappa} \rangle_{\mathbf{k}\mathbf{k}'}^2 \equiv \langle (\alpha_{\mu\nu}^{\kappa})_{\mathbf{k}} \rangle \langle (\alpha_{\mu\nu}^{\kappa})_{\mathbf{k}'} \rangle$ . With this notation, the expectation value of the Hubbard interaction becomes<sup>30</sup>

$$\langle H_{\text{Hubb}} \rangle = \frac{16U}{N} \sum_{\mathbf{k}, \mathbf{k}'}'' \underbrace{\langle \alpha_{0i}^3 \rangle_{\mathbf{k}\mathbf{k}'}}_{\text{SC-CDW}} - \underbrace{\langle \alpha_{i0}^3 \rangle_{\mathbf{k}\mathbf{k}'}}_{\text{AF}} + \underbrace{\langle \alpha_{0i}^1 \rangle_{\mathbf{k}\mathbf{k}'}}_{\text{SC' fill}} - \underbrace{\langle \alpha_{i0}^1 \rangle_{\mathbf{k}\mathbf{k}'}}_{\text{FM}}, \quad (18)$$

where the index  $i$  is summed from 1 to 3. The terms representing the mixed superconducting and charge-density wave (SC-CDW), antiferromagnetic (AF), and ferromagnetic (FM) ordering are underbraced. The third ( $z$ ) component of the SC'-fill term is recognized as the filling while the  $x$  and  $y$  components represent the real and imaginary part of a kind of staggered superconductor (SC'). This term together with the first are the analogs of the FM and AF states under the change of sign of  $U$ . We find numerically that the order parameter for SC' is always zero for the interaction parameters that we consider.

$$\langle H_{\text{Heis}} \rangle = \frac{16J}{N} \sum_{\mathbf{k}, \mathbf{k}'}'' 2 \underbrace{\langle \alpha_{i0}^1 \rangle_{\mathbf{k}\mathbf{k}'}}_{\text{FM}}^2 - 2 \underbrace{\langle \alpha_{i0}^3 \rangle_{\mathbf{k}\mathbf{k}'}}_{\text{AF}}^2 + \frac{1}{4} (\gamma_{\mathbf{k}} \gamma_{\mathbf{k}'} + \eta_{\mathbf{k}} \eta_{\mathbf{k}'}) \left( -3 \underbrace{\langle \alpha_{00}^1 \rangle_{\mathbf{k}\mathbf{k}'}}_{\text{hop}}^2 - 3 \underbrace{\langle \alpha_{0i}^2 \rangle_{\mathbf{k}\mathbf{k}'}}_{\text{SC-CDW}}^2 + \underbrace{\langle \alpha_{i0}^2 \rangle_{\mathbf{k}\mathbf{k}'}}_{\text{spin nem.}}^2 + \langle \alpha_{ij}^1 \rangle_{\mathbf{k}\mathbf{k}'}^2 \right) + \frac{1}{2} (\zeta_{k_x} \zeta_{k'_x} + \zeta_{k_y} \zeta_{k'_y}) \left( -3 \langle \alpha_{00}^3 \rangle_{\mathbf{k}\mathbf{k}'}^2 - 3 \langle \alpha_{0i}^0 \rangle_{\mathbf{k}\mathbf{k}'}^2 + \langle \alpha_{i0}^0 \rangle_{\mathbf{k}\mathbf{k}'}^2 + \underbrace{\langle \alpha_{ij}^3 \rangle_{\mathbf{k}\mathbf{k}'}}_{p \text{ wave}}^2 \right). \quad (19)$$

From this form we see that the Heisenberg term renormalizes the hopping and also affects the antiferromagnetic and ferromagnetic ordering. Apart from these terms, the most interesting term is the  $\alpha_{0i}^2$  term representing superconducting and CDW ordering. This term is split into two irreps,  $A_1$  and  $B_1$ , corresponding to  $\gamma_{\mathbf{k}}$  and  $\eta_{\mathbf{k}}$ . The  $A_1$  part gives rise to “extended  $s$ -wave superconductivity” in certain regions of parameter space. The  $B_1$  part introduces  $d$ -wave superconductivity, and the  $z$  component of this part is recognized as an orbital antiferromagnet. We also recognize the  $B_1$  representation of the  $\alpha_{i0}^2$  term, which represents a spin nematic state with the order parameter  $\langle c_{\mathbf{k},\alpha}^\dagger c_{\mathbf{k},\beta} \rangle = i\eta_{\mathbf{k}} \sigma_{\alpha\beta} \cdot \mathbf{d}$ , where  $\mathbf{d}$  is a real vector. Finally, there is a term representing  $p$ -wave superconductivity and since it is odd under parity it belongs to the two-dimensional  $E$  representation. Some of the other terms may have been discussed in the literature but, since we have found them not to be energetically favored, we do not discuss them further.

In addition, the full Hamiltonian gives a term that shifts the chemical potential, and the Hubbard and chemical-potential terms produce constants that shift the energy. These terms have no significance in our analysis and they are neglected in the following.

In collecting all these terms, it is useful to write the expectation value of the Hamiltonian in the following generic form:

To make a more systematic investigation of all order parameters, we note that the Hubbard model on the 2D square lattice has the point-group symmetry  $C_{4v}$ , which has four 1D irreps ( $A_1$ ,  $A_2$ ,  $B_1$ , and  $B_2$ ) and one 2D irrep ( $E$ ) (see Appendix A). The total symmetry is hence  $C_{4v} \times \text{SU}(2) \times \text{SU}(2)$ , and it is possible to perform a complete classification of the order parameters.<sup>8</sup>

Since the Hubbard interaction is on-site, the interaction coefficients are independent of  $\mathbf{k}$  and all the prefactors of the Hubbard term belong to the  $A_1$  irrep. Another basis function for this representation is  $\gamma_{\mathbf{k}} = \cos(k_x) + \cos(k_y)$ , which occurs in the hopping and Heisenberg terms and in “extended  $s$ -wave” superconductivity. The Heisenberg term has also components in the  $B_1$  and the  $E$  representations. The  $B_1$  terms (odd under  $k_x \leftrightarrow k_y$ ) have the  $\mathbf{k}$ -dependence  $\eta_{\mathbf{k}} = \cos(k_x) - \cos(k_y)$  and the two basis functions of the  $E$  representation (odd under parity,  $\mathbf{k} \rightarrow -\mathbf{k}$ ) are  $\zeta_{k_x} = \sin(k_x)$  and  $\zeta_{k_y} = \sin(k_y)$ . The expectation value of the Heisenberg term reads, in its whole glory,

$$\langle H \rangle = \sum_{l,m,\mathbf{k}}'' a_{l,m} \beta_{\mathbf{k}}^l \langle \alpha_{\mathbf{k}}^m \rangle + \sum_{l,m,\mathbf{k},\mathbf{k}'}'' b_{l,m} \beta_{\mathbf{k}}^l \beta_{\mathbf{k}'}^l \langle \alpha_{\mathbf{k}}^m \rangle \langle \alpha_{\mathbf{k}'}^m \rangle, \quad (20)$$

where  $a_{l,m}$  and  $b_{l,m}$  are coefficients of the linear and quadratic terms, respectively, and  $\beta_{\mathbf{k}}^l = 1, \gamma_{\mathbf{k}}, \eta_{\mathbf{k}}, \dots$  are trigonometric prefactors from various irreps of the point group  $C_{4v}$ . The index  $l$  labels the irreps of  $C_{4v}$ , while the index  $m$  labels the irreps of  $\text{SU}(2) \times \text{SU}(2)$ .

## V. INCORPORATING THE SPIRAL PHASES IN THE HAMILTONIAN

The most important unanswered question is what happens when the electronic density deviates from half-filling? A widely discussed scenario is that the antiferromagnetic state adjusts to incorporate the excess electrons and changes into a spiral phase—an antiferromagnetic phase whose order parameter shows a spiral spatial distribution. Given that the spiral antiferromagnet is the energetically preferred phase in some other mean-field calculations, we must clearly incorporate this scenario in our analysis. Unfortunately, spiral states cannot be directly generated by the Bogoliubov transformations we have used so far. We therefore generalize our method by imposing a spiral twist of the quantization axis on

the Hamiltonian *before* the mean-field approximation is applied.

To describe any spiral we need a 2D vector  $\mathbf{q}$  in the plane, which controls the direction and pitch of the spiral spin wave, and a 3D unit vector  $\mathbf{\Omega}$  which defines the axis around which the spin is twisted. The spin-twisting canonical transformation is then generated by the operator

$$\begin{pmatrix} c_{\mathbf{r},\uparrow}^\dagger & c_{\mathbf{r},\downarrow}^\dagger \end{pmatrix} \exp[i(\mathbf{q} \cdot \mathbf{r})(\mathbf{\Omega} \cdot \boldsymbol{\sigma})] \begin{pmatrix} c_{\mathbf{r},\uparrow} \\ c_{\mathbf{r},\downarrow} \end{pmatrix}, \quad (21)$$

where  $\boldsymbol{\sigma}$  is the vector of Pauli matrices. This canonical transformation is easily written as a unitary transformation of the creation/annihilation operators,

$$\begin{pmatrix} c_{\mathbf{r},\uparrow}^\dagger \\ c_{\mathbf{r},\downarrow}^\dagger \end{pmatrix} \rightarrow [\cos(\mathbf{q} \cdot \mathbf{r})\mathbb{1} + i \sin(\mathbf{q} \cdot \mathbf{r})\mathbf{\Omega} \cdot \boldsymbol{\sigma}] \begin{pmatrix} c_{\mathbf{r},\uparrow}^\dagger \\ c_{\mathbf{r},\downarrow}^\dagger \end{pmatrix}. \quad (22)$$

Since the Hamiltonian is invariant under global spin rotations the direction of  $\mathbf{\Omega}$  can be arbitrarily set to be along  $\hat{z}$ .

When applying this spiral spin transformation to  $H$ , the Hubbard interaction is invariant since it is spin-rotation invariant and on site, but the hopping term transforms into  $H_0^q = \sum_{\mathbf{k}} \epsilon_{\mathbf{k}}(n_{\mathbf{k}+\mathbf{q},\uparrow} + n_{\mathbf{k}-\mathbf{q},\downarrow})$ , which, using our operator definitions, is written as

$$\begin{aligned} \langle H_0^q \rangle &= -2t \sum''_{\mathbf{k},n=x,y} 8[\cos(q_n) \cos(k_n) \langle (\alpha_{00}^1)_{\mathbf{k}} \rangle \\ &\quad + \sin(q_n) \sin(k_n) \langle (\alpha_{30}^0)_{\mathbf{k}} \rangle]. \end{aligned} \quad (23)$$

The Heisenberg term transforms into  $H_{\text{Heis}}^q = J \sum_{\langle \mathbf{R}, \mathbf{R}' \rangle} \vec{S}_{\mathbf{R}} \cdot \vec{S}_{\mathbf{R}'} \cos[2\mathbf{q} \cdot (\mathbf{R} - \mathbf{R}')] + 2S_{\mathbf{R}}^z S_{\mathbf{R}'}^z \sin^2[\mathbf{q} \cdot (\mathbf{R} - \mathbf{R}')]$ , where  $S_{\mathbf{R}}^z$  denotes the  $z$  component of the local spin operator at site  $\mathbf{R}$ . Using the same notation as in Eqs. (18) and (19) with the extension that  $\iota$  is an index that is summed over 1 and 2 only, the Heisenberg expectation value is

$$\begin{aligned} \langle H_{\text{Heis}}^q \rangle &= \frac{16J}{N} \sum''_{\substack{\mathbf{k}, \mathbf{k}' \\ n=x,y}} \left[ \langle \alpha_{30}^1 \rangle_{\mathbf{k}\mathbf{k}'}^2 - \langle \alpha_{30}^3 \rangle_{\mathbf{k}\mathbf{k}'}^2 + \cos(q_n) [\langle \alpha_{i0}^1 \rangle_{\mathbf{k}\mathbf{k}'}^2 - \langle \alpha_{i0}^3 \rangle_{\mathbf{k}\mathbf{k}'}^2] + \frac{1}{2} \cos(k_n) \cos(k'_n) \right. \\ &\quad \times \left\{ -[1 + 2 \cos(2q_n)] [\langle \alpha_{00}^1 \rangle_{\mathbf{k}\mathbf{k}'}^2 + \langle \alpha_{0i}^2 \rangle_{\mathbf{k}\mathbf{k}'}^2] + \langle \alpha_{i0}^2 \rangle_{\mathbf{k}\mathbf{k}'}^2 + \langle \alpha_{ii}^1 \rangle_{\mathbf{k}\mathbf{k}'}^2 + [2 \cos(2q_n) - 1] [\langle \alpha_{30}^2 \rangle_{\mathbf{k}\mathbf{k}'}^2 + \langle \alpha_{3i}^1 \rangle_{\mathbf{k}\mathbf{k}'}^2] \right\} \\ &\quad + \sin(k_n) \sin(k'_n) \left\{ -[1 + 2 \cos(2q_n)] [\langle \alpha_{00}^3 \rangle_{\mathbf{k}\mathbf{k}'}^2 + \langle \alpha_{0i}^0 \rangle_{\mathbf{k}\mathbf{k}'}^2] + \langle \alpha_{i0}^0 \rangle_{\mathbf{k}\mathbf{k}'}^2 + \langle \alpha_{ii}^3 \rangle_{\mathbf{k}\mathbf{k}'}^2 \right. \\ &\quad \left. \left. + [2 \cos(2q_n) - 1] [\langle \alpha_{30}^0 \rangle_{\mathbf{k}\mathbf{k}'}^2 + \langle \alpha_{3i}^3 \rangle_{\mathbf{k}\mathbf{k}'}^2] \right\} \right]. \end{aligned} \quad (24)$$

The large number of terms in this expression is due to the broken spin-rotational and point-group symmetries.

## VI. SOLVING FOR THE STATE OF LOWEST FREE ENERGY

### A. Self-consistent equations at finite temperature

In the spirit of standard BCS theory we introduce the reduced Hamiltonian

$$H = \sum''_{l,m,\mathbf{k}} a_{l,m} \beta_{\mathbf{k}}^l \alpha_{\mathbf{k}}^m + \sum''_{l,m,\mathbf{k},\mathbf{k}'} b_{l,m} \beta_{\mathbf{k}}^l \beta_{\mathbf{k}'}^l \alpha_{\mathbf{k}}^m \alpha_{\mathbf{k}'}^m, \quad (25)$$

which has the generic expectation value given in Eq. (20). We also define the mean-field order parameters (gap functions)

$$\Delta_{l,m} = \sum''_{\mathbf{k}} \beta_{\mathbf{k}}^l \langle \alpha_{\mathbf{k}}^m \rangle. \quad (26)$$

Using the assumption that the fluctuations in the operators  $\alpha_{\mathbf{k}}^m$  from their mean-field values are small, we substitute  $\alpha_{\mathbf{k}}^m = (\alpha_{\mathbf{k}}^m - \langle \alpha_{\mathbf{k}}^m \rangle) + \langle \alpha_{\mathbf{k}}^m \rangle$  into  $H$  in Eq. (25), drop terms quadratic in  $(\alpha_{\mathbf{k}}^m - \langle \alpha_{\mathbf{k}}^m \rangle)$ , and find the mean-field Hamiltonian  $H_{\text{mf}}$ ,

$$H_{\text{mf}} = \sum''_{l,m,\mathbf{k}} (a_{l,m} + 2b_{l,m} \Delta_{l,m}) \beta_{\mathbf{k}}^l \alpha_{\mathbf{k}}^m - \sum_{l,m} \Delta_{l,m}^2. \quad (27)$$

Aside from a constant that is unimportant in this discussion,  $H_{\text{mf}}$  can be recast in the form

$$H_{\text{mf}} = \frac{1}{8} \sum''_{\mathbf{k}} \text{Tr}[h(\mathbf{k})(\Psi_{\mathbf{k}}^\dagger \otimes \Psi_{\mathbf{k}})], \quad (28)$$

where

$$h(\mathbf{k}) = \sum_{l,m} (a_{l,m} + 2b_{l,m} \Delta_{l,m}) \beta_{\mathbf{k}}^l B_m. \quad (29)$$

Introducing the matrix of expectation values  $f_{\mathbf{k}} \equiv \langle (\Psi_{\mathbf{k}}^\dagger \otimes \Psi_{\mathbf{k}}) \rangle$ , it follows from Eqs. (16) and (26) that

$$\Delta_{l,m} = \frac{1}{8} \sum''_{\mathbf{k}} \beta_{\mathbf{k}}^l \text{Tr}(B_m f_{\mathbf{k}}). \quad (30)$$

To evaluate  $f_{\mathbf{k}}$  we note that the mean-field Hamiltonian is bilinear in  $\Psi_{\mathbf{k}}^\dagger$  and can be diagonalized,  $H_{\text{mf}} = \sum''_{\alpha,\mathbf{k}} \epsilon_{\alpha}(\mathbf{k})(\chi_{\mathbf{k}}^\dagger)^\alpha (\chi_{\mathbf{k}})^\alpha$ , by the canonical transformation  $\chi_{\mathbf{k}}^\dagger = U_{\mathbf{k}} \Psi_{\mathbf{k}}^\dagger$ , where  $U_{\mathbf{k}}$  is an  $U(8)$  matrix. Standard arguments from statistical mechanics give in the diagonal case

$$\langle (\chi_{\mathbf{k}}^\dagger \otimes \chi_{\mathbf{k}})_{\alpha, \gamma} \rangle = (1 + e^{\beta \epsilon_\alpha(\mathbf{k})})^{-1} \delta_{\alpha\gamma} \quad (31)$$

( $\beta$  is the inverse temperature,  $\beta = 1/k_B T$ ) which, when transformed back to the operators  $\Psi_{\mathbf{k}}$ , results in

$$f_{\mathbf{k}} = \langle (\Psi_{\mathbf{k}}^\dagger \otimes \Psi_{\mathbf{k}}) \rangle = (1 + e^{\beta h(\mathbf{k})})^{-1}. \quad (32)$$

Equations (29), (30), and (32) constitute the self-consistent equations to be solved for  $\Delta_{l,m}$ . The solutions extremize the free energy  $F$ ,

$$F = \langle H \rangle - TS, \quad (33)$$

where  $\langle H \rangle$  now includes the chemical potential, and where  $S$  is the entropy. If more than one solution is found, then the one with the minimal value of  $F$  is the physical one. To calculate  $F$ , both terms in Eq. (33) must be explicitly evaluated. The evaluation of  $\langle H \rangle$  is straightforward—using Eq. (20) we see that it is equal to

$$\langle H \rangle = \sum_{l,m} (a_{l,m} \Delta_{l,m} + b_{l,m} \Delta_{l,m}^2). \quad (34)$$

The entropy is in turn given by

$$S = -k_B \sum_{\mathbf{k}} \text{Tr} [f_{\mathbf{k}} \ln f_{\mathbf{k}} + (1 - f_{\mathbf{k}}) \ln (1 - f_{\mathbf{k}})], \quad (35)$$

where  $f_{\mathbf{k}}$  is the matrix of expectation values defined in Eq. (32).

## B. Zero temperature

At zero temperature, the variational state gives an approximate ground state  $|G\rangle$  and the thermal expectation values evolve into expectation values with respect to this ground state, i.e.,  $\langle (\Psi_{\mathbf{k}}^\dagger \otimes \Psi_{\mathbf{k}}) \rangle$  is replaced by  $\langle G | \Psi_{\mathbf{k}}^\dagger \otimes \Psi_{\mathbf{k}} | G \rangle$ . The zero-temperature self-consistent equations are obtained from Eq. (30) in the limit  $\beta \rightarrow \infty$ .

Combining the facts that the ground state is the vacuum state for the quasiparticles and that the first (last) four elements of  $\chi_{\mathbf{k}}$  are annihilation (creation) operators, we can identify the diagonal matrix  $g = \langle G | (\chi_{\mathbf{k}}^\dagger \otimes \chi_{\mathbf{k}}) | G \rangle$ . Its diagonal entries are  $(0, 0, 0, 0, 1, 1, 1, 1)$ , and from Eq. (31) with  $\beta \rightarrow \infty$  it follows that four of the eigenvalues of  $h(\mathbf{k})$  must be negative and the rest positive. We then solve for the unitary matrices  $U_{\mathbf{k}}$  that diagonalize the  $h(\mathbf{k})$ 's defined in Eq. (29), in such a way that the eigenvalues in the diagonal matrices  $D_{\mathbf{k}}$  are in descending order. The self-consistent equations to be iterated are then Eq. (29) and

$$\Delta_m = \frac{1}{8} \sum_{\mathbf{k}} \beta_{\mathbf{k}}^m \text{Tr} (B_m U_{\mathbf{k}}^\dagger g U_{\mathbf{k}}), \quad (36a)$$

$$D_{\mathbf{k}} = U_{\mathbf{k}} h(\mathbf{k}) U_{\mathbf{k}}^\dagger. \quad (36b)$$

## C. An alternative set of equations for the ground state at half-filling

The self-consistent equations must be solved numerically. Although the equations are formally simple, it is

quite challenging to numerically carry out a search of the solution space. We therefore present an alternative method to find the ground state, and use it to derive a theorem of stability of the superconducting and the antiferromagnetic solutions at half-filling for some regimes of  $U$  and  $J$ .

Naïvely, the expectation value of the Hamiltonian, Eq. (20), is a simple quadratic form and one should just find its minimum. However, since the expectation values  $\langle \alpha_{\mathbf{k}}^m \rangle$  are constrained by the fact that they represent expectation values of fermion operators, the terms cannot be independently varied, and there are constraints on the set of  $\langle \alpha_{\mathbf{k}}^m \rangle$ . These restrictions were automatically satisfied in the previous analysis, since  $\alpha_{\mathbf{k}}^m$  was explicitly computed through a canonical transformation. Another way to proceed is to try to find a constrained quadratic minimum directly without first calculating a canonical transformation.

To express the fermionic constraints, we define the following matrix:

$$A_{\mathbf{k}} = \sum_{\substack{m \neq m' \\ m, m' \neq 0}} \langle \alpha_{\mathbf{k}}^m \rangle \langle \alpha_{\mathbf{k}}^{m'} \rangle \{B_m, B_{m'}\}, \quad (37)$$

where  $\{A, B\}$  denotes the anticommutator  $\{A, B\} \equiv AB + BA$ . The matrix  $B_0 \equiv B_{00}^0 = -\mathbb{1}$  that is excluded from the sum is the only basis matrix with nonzero trace. First we state the lemma that reformulates the problem of minimizing the energy.

**Lemma 1.** *The restrictions on the expectation values  $\langle \alpha_{\mathbf{k}}^m \rangle$  for the variational solutions of Eq. (20) are  $\sum_m \langle \alpha_{\mathbf{k}}^m \rangle^2 = \frac{1}{2}$ ,  $\langle (\alpha_{00}^0)_{\mathbf{k}} \rangle = -\frac{1}{2}$ , and  $A_{\mathbf{k}} = 0 \forall \mathbf{k}$ .*

This lemma is proved in Appendix B. The importance of the lemma is that it shows that the minimization problem of Eq. (20) is a quadratic minimum subject to quadratic constraints. This enables us to search for minima of the *unconstrained* problem, which, if they are found to satisfy the constraints, must also be minima of the constrained problem. A class of such solutions are introduced in the following theorem (proved in Appendix B) and corollary.

**Theorem 1.** *Consider the Hamiltonian in Eq. (20) with fixed coefficients  $a_{l,m}$  and  $b_{l,m}$ . Define  $\mathcal{N}$  as the subset of purely quadratic and irreducible terms,  $\mathcal{N} = \{m : a_{l,m} = 0 \forall l, b_{l,m} = b_m \delta_{l, l(m)}\}$ , where  $l(m)$  is a function which attaches one single  $l$  to each  $m$ . Assume there exists an  $\tilde{m} \in \mathcal{N}$ , such that  $(b_{\tilde{m}} < 0$  and  $b_{\tilde{m}} |\beta_{\mathbf{k}}^{l(\tilde{m})} \beta_{\mathbf{k}'}^{l(\tilde{m})}| < b_m |\beta_{\mathbf{k}}^{l(m)} \beta_{\mathbf{k}'}^{l(m)}| \forall \mathbf{k}, \mathbf{k}', \forall m \in \mathcal{N} \setminus \{\tilde{m}\})$ . If  $(\langle \alpha_{\mathbf{k}}^m \rangle = 0 \forall \mathbf{k}, \forall m \in \mathcal{N} \setminus \{\tilde{m}\})$  is a sufficient condition for  $(A_{\mathbf{k}} = 0 \forall \mathbf{k})$ , then the same  $\langle \alpha \rangle$ 's will be zero also in the minimizing solution of the constrained problem.*

In the case of half-filling the following corollary now follows for the two important cases of antiferromagnetic and  $s$ -wave superconducting ordering.<sup>38</sup>

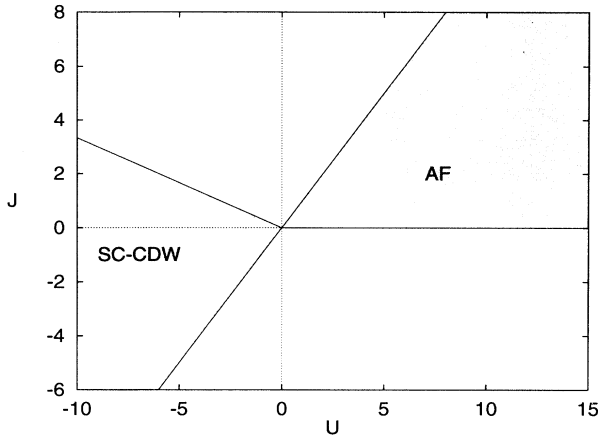


FIG. 2. The low energy states of the extended Hubbard model according to Corollary 1 is shown in grey. The white areas are indeterminate from the corollary, and the phases here must be computed numerically.

**Corollary 1.** *The state of lowest energy at half-filling ( $\mu = 0$ ) for the Hamiltonian ( $H = H_0 + H_{\text{Hubb}} + H_{\text{Heis}}$ ) in Eqs. (17), (18), and (19) is AF ( $\langle \alpha_{i0}^2 \rangle \neq 0$ ) if  $0 < J < U$ , and  $s$ -wave SC-CDW ( $\langle \alpha_{0i}^2 \rangle \neq 0$ ) if  $U < J < -U/3$ .*

The theorem follows by making two observations. First, the possible low-energy states follow from Theorem 1 by inspection of the prefactors of the quadratic terms in the Hamiltonian, and by verifying that  $A_{\mathbf{k}} = 0$  if all  $\langle \alpha \rangle$ 's are zero except the hopping ( $\alpha_{00}^1$ ) and either  $\langle \alpha_{i0}^2 \rangle$  or  $\langle \alpha_{0i}^2 \rangle$ . Secondly, we observe that the problem that results by setting all other order parameters to zero is analogous to the ordinary  $s$ -wave SC case, where it is well known that any attractive interaction results in a finite order parameter.

We further note that there are two degenerate superconductivity solutions if the constraints are disregarded. One is the ordinary  $s$ -wave superconductor, and the other is the staggered superconductor. However, the latter is ruled out by the fact that the constraint  $A_{\mathbf{k}} = 0$  is not fulfilled. Apart from predicting these low energy states, Theorem 1 also proves the stability of these phases with respect to small perturbations to the Hamiltonian. Since the ferromagnetic state has  $A_{\mathbf{k}} \neq 0$ , ferromagnetic ordering and nonzero hopping cannot be present simultaneously, at least not at the same location in  $\mathbf{k}$  space. The predictions of the corollary are illustrated in Fig. 2.

It is interesting to compare our predictions with the model extended by the correlated hopping term in Eq. (6) with  $X = t$  since there exists a rigorous criterion for when the SC state is the ground state of that model.<sup>23</sup> According to that criterion the system is superconducting when  $-8|t| > U < J < -U/3$ , which for sufficiently small  $U$  coincides exactly with our boundaries.

## VII. NUMERICAL METHODS

To find the phase at a  $(U, J, \mu, T)$  point in a phase diagram, we choose an initial value of the pitch vector

$\mathbf{q}$ , solve the self-consistent equations Eqs. (29), (30), and (32) numerically, and calculate  $F(\mathbf{q})$  using Eqs. (34) and (35).

The pitch vector  $\mathbf{q}$  is then varied to find which  $\mathbf{q}$  gives the solution to the self-consistent equations with the lowest value of  $F(\mathbf{q})$ . The nonzero mean-field order parameters  $\Delta_{l,m}$  defines, together with  $\mathbf{q}$ , the particular phase for the  $(U, J, \mu, T)$  point in parameter space.

Complete phase diagrams are obtained by the following two steps.

The parameters  $(U, J, \mu, T, \mathbf{q})$  are swept, with an initial set of  $\Delta_m$ 's generated at random and the self-consistent equations are iterated until a fixed point is reached. This gives us a rough picture of the states that are present in the phase diagram.

The accuracy of the boundaries between the phases in the phase diagram is improved. Here the self-consistent equations are solved using Broyden's method,<sup>39</sup> which is often more efficient than the previous iterative method.

To find  $\Delta_{l,m}$  for a particular value of  $\mathbf{q}$ , we cover the reduced Brillouin zone by a discrete lattice. Care has to be taken not to break any of the symmetries of the problem. Figure 1 shows how a 32-point lattice is laid out. The most time-consuming numerical step is to diagonalize the  $8 \times 8$  matrix in the argument of the exponential function in Eq. (32) at every  $\mathbf{k}$  point; this must be done for each iteration.

Choosing random order parameters as initial conditions for recursion is useful when there is no *a priori* information about the expected solutions of the self-consistent equations. A complication of this method, however, is that the iteration tends to fall into cycles. We cured this by including a tail of exponentially damped previous iterates at each step. Sometimes, the procedure still did not converge, and several initial points must be used before a fixed point was found.

To obtain a complete  $\mu$ - $T$  phase diagram for fixed  $U$  and  $J$ , we cover the  $(\mu, T, \mathbf{q})$  space with roughly 1500 points, and repeat the iterative procedure 10 times. On an ordinary workstation it takes of the order of a week of CPU time to trace out the phase diagram using 98 points in the reduced Brillouin zone and solving the self-consistent equations to an accuracy of 1%. Of course, solutions could be missed by chance since we use random initial guesses, and phases occurring in narrow regions of the phase space could be missed since the parameter space is not covered with a fine enough mesh.

After the different phases have been identified, we obtain more accurate solutions of the self-consistent equations using Broyden's method. This method cannot be used from the beginning since the initial guess has to be close to the final answer for the method to converge. The method is also slow if the number of order parameters is very large. Here, we therefore eliminate from the Hamiltonian all order parameters that are known to be zero in the corresponding regions.

If the state of lowest free energy has  $\mathbf{q} = 0$  the minimizing solution can be obtained directly by Broyden's method, and in this case the phase boundaries are located to high accuracy, generally by using 800 points in the reduced Brillouin zone.



If  $\mathbf{q}$  is nonzero, there is the extra problem of minimizing the free energy with respect to  $\mathbf{q}$ . We do this by using Broyden's method for solving the self-consistent equations and extending it with a simple numerical algorithm that also minimizes in  $\mathbf{q}$  using Brent's method.<sup>39</sup> To obtain results within reasonable computing time, most of the spiral spin wave calculations have been performed using a 392-point lattice in the reduced Brillouin zone.

In order to allow for the most general spiral solutions, no restrictions should be imposed on the spiral spin wave parameter  $\mathbf{q}$ , but that would make the problem numerically unmanageable. Instead we have focused on the question of whether the low-energy state is a spiral spin wave or not. Assuming the spiral spin wave not to break the lattice symmetries completely, the quantization axis  $\mathbf{q}$  could be twisted either in the (1,1) or (1,0) direction. We further concentrated on the latter case case,  $\mathbf{q} = (q, 0)$ , since it turned out to give a slightly lower free energy than the diagonal twist in some regions of the phase diagram.

## VIII. PHASE DIAGRAMS

In order to present a set of complete phase diagrams for the extended Hubbard model, we would have to probe all combinations of values of the four parameters  $U$ ,  $J$ , filling (or  $\mu$ ), and  $T$ . This is an infeasible task, and we restrict ourselves to certain cross sections that we hope to capture generic behavior. Due to the particle-hole symmetry as  $\mu \rightarrow -\mu$ , we restrict our phase diagrams to hole doping ( $\mu < 0$ ). We can further set  $t = 1$  without loss of generality.

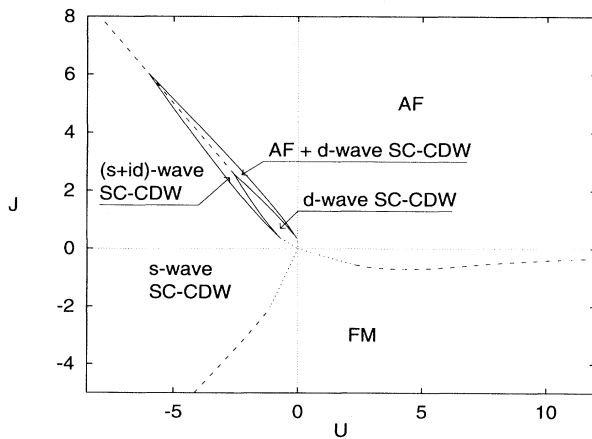


FIG. 3. Phase diagram at half-filling and zero temperature as a function of  $J$  and  $U$ . Second-order phase boundaries are drawn as full lines, while first-order phase boundaries are drawn as dashed lines. The dotted lines are extrapolations of the numerically derived full (dashed) line phase boundaries.

### A. Zero temperature and half-filling

The most fundamental cross section is ( $T = 0, \mu = 0$ ) corresponding to the ground state of the half-filled extended Hubbard model in Fig. 3. In this case, when  $U$  and  $J$  are both positive, as well as for a region of negative  $U$ , the antiferromagnetic state forms a numerically very stable solution. This is consistent with Corollary 1. The corollary further indicates a region (SC-CDW) of degenerate  $s$ -wave SC and charge-density-wave state, which is confirmed by the numerical simulations for negative  $U$  and intermediate  $J$ .

An interesting feature occurring in a region outside the validity of the assumptions of Corollary 1, but which is numerically very robust, is the tongue of  $d$ -wave SC-CDW, ( $s+id$ )-wave SC-CDW, and ( $d$ -wave SC-CDW)+AF between the AF and the  $s$ -wave states. The  $d$ -wave order parameter is dominant along the center line of the tongue while it vanishes at the boundaries. Numerically we also see that the  $s$ - and  $d$ -wave order parameters form parallel pseudospin vectors, and the explicit form of the base matrices of these vectors indicate that the mixed state breaks time reversal symmetry, i.e., it is an  $s+id$  state. This is consistent with the constraint  $A_{\mathbf{k}} = 0$  in Lemma 1, since the constraint requires the two pseudospin vectors to be parallel unless some other order parameter is nonzero.

The ferromagnetic (FM) phase that is seen for negative  $J$  is just barely numerically stable close to the phase boundaries. It is, however, quite stable deeper inside the FM region where the ferromagnetic state gets saturated. Our observations do not contradict rigorous criteria for the saturated zone.<sup>40</sup> The numerical difficulties near the FM phase boundaries can be understood by the constraint conditions discussed in Lemma 1. Since, in the absence of a third order parameter, hopping and FM order cannot exist simultaneously at the same point in the Brillouin zone, there will be distinct regions in  $\mathbf{k}$  space. The FM ordering occurs close to the Fermi surface, while the hopping expectation value is finite near the origin in reciprocal space. The sharp boundary between the two regions results in discontinuities in the numerical solution.

### B. Finite temperature

We now turn to phase diagrams at nonzero temperature and variable filling for some particular fixed values of  $U$  and  $J$ . Estimates using physical models for the high- $T_c$  materials have suggested that  $U$  should be of the order 5 with  $J$  much smaller. The relevance of such estimates for the present calculation is questionable since they were made for models of high- $T_c$  materials that include other types of interactions such as nearest-neighbor charge repulsion. Moreover, a large fraction of our Heisenberg term could be considered as coming from effective second-order corrections to the Hubbard interaction, which are otherwise neglected in our mean-field approach. Therefore, we concentrate on parameter val-

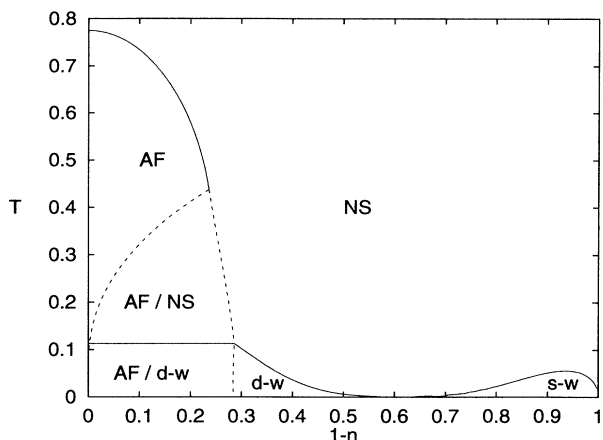


FIG. 4. Phase diagram for  $U = 0.5$ ,  $J = 2$ . Second-order phase transitions are drawn as full lines, while the boundaries of regions with phase separation are drawn as dashed lines. The regions of phase separation are denoted A/B where A and B are the two coexisting phases. Regions of  $s$ -wave and  $d$ -wave SC are indicated by  $s$ -w and  $d$ -w, respectively.

ues that give interesting phenomena.

There are two features that we are particularly interested in exploring. The first is  $d$ -wave superconductivity, and the second is spiral spin waves. To keep some connection to high- $T_c$  materials, we require the model to be antiferromagnetic at half-filling, and therefore  $U$  and  $J$  should be positive. In order to study  $d$ -wave superconductivity,  $U$  should not be too large. The spiral spin-wave states, on the other hand, have been observed for the pure Hubbard model with intermediate  $U$ , and in this case  $J$  should be zero or at least small.

We start out by investigating the phase diagram for  $U = 0.5$  and  $J = 2$  which contains a zone of  $d$ -wave superconductivity (see Fig. 4). The system is antiferromagnetic close to half-filling. This state persists up to the Néel temperature, where there is a second-order phase transition to the normal state (NS) that has no broken symmetry. At low temperatures and moderate doping, we have a  $d$ -wave superconductor which is separated from the antiferromagnet by a first-order phase transition. For temperatures higher than the SC critical temperature, there is a first-order phase transition between the antiferromagnet and the normal state. This first-order boundary terminates at higher temperatures at a critical point, where the transition becomes second order. No qualitative differences between this phase diagram and that for  $U = 0$  is observed.

Both antiferromagnetic phases and  $s$ - and  $d$ -wave superconductors have been observed in other calculations.<sup>12</sup> Those studies did not consider the possibility that the phase transition could be first order, but by carefully comparing the free energies we have observed this type of transition between the AF and the  $d$ -wave SC states at low temperature. If, as in our model, the total electron number is fixed, the first-order phase transition results in phase separation.

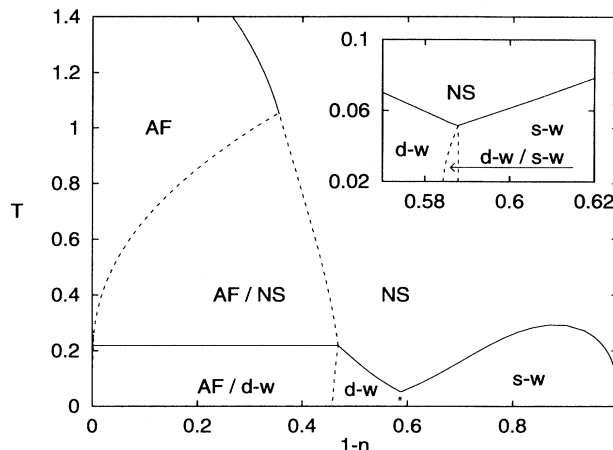


FIG. 5. Phase diagram for  $U = 0$  and  $J = 4$ . The  $d$ -wave and  $s$ -wave superconducting regions are separated by a first-order phase transition, with a very narrow coexistence region. The inset shows a magnification of the coexistence region.

By increasing  $J$  and  $U$ , the antiferromagnetic region is enhanced. The  $d$ -wave zone grows with increasing  $J$ , but is also shifted to larger doping as the antiferromagnetic region expands at the same time. The overall size of the SC region in the  $T$ - $\mu$  phase diagram is insensitive to a change in  $U$ . The  $s$ -wave superconducting zone is also enhanced by larger  $J$ , while it diminishes if  $U$  is increased too much. It should also be noted that the AF and the  $s$ -wave SC regions gain more from an increase in  $J$  than the  $d$  wave regions do. This is illustrated in Fig. 5, where the phase diagram for  $U = 0$  and  $J = 4$  is exhibited. If  $J$  is sufficiently large, we expect the  $d$  wave to disappear in favor of the  $s$ -wave SC and the AF phases.

For large  $U$  and small  $J$ , spiral spin waves appear as shown in Fig. 6 for  $J = 0$ . The phase diagram is shown in Fig. 6, where SSW indicates the spiral spin wave with the

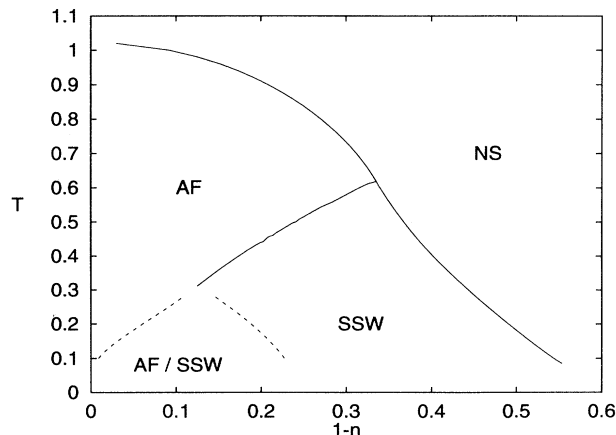


FIG. 6. Phase diagram for  $U = 5$  and  $J = 0$ . The spiral spin wave with pitch  $(\pi - q, \pi)$  is denoted SSW.

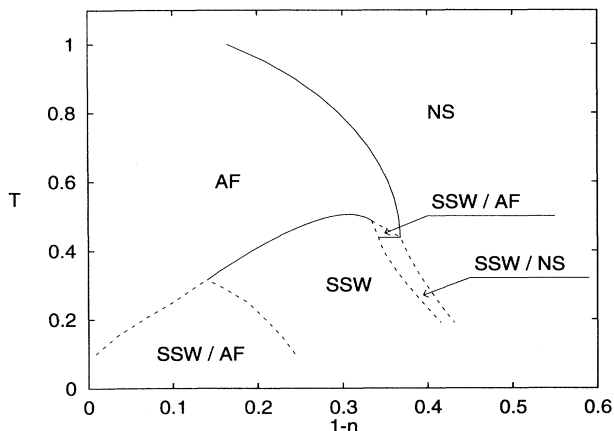


FIG. 7. Phase diagram for  $U = 5$ ,  $J = 0.1$ . The SSW has pitch  $(\pi - q, \pi)$ .

pitch  $(\pi - q, \pi)$ , which is obtained by applying the twist  $\mathbf{q} = (1, 0)q$  to the AF  $(\pi, \pi)$  state. At low temperature, the SSW state is separated from the AF state by a first-order phase transition with a wide coexistence region as a function of density. For more elevated temperatures, the separation line becomes second-order and here the spiral pitch parameter  $q$  goes to zero as the phase boundary is approached. On the contrary, along the phase transition from the SSW to the normal state the spiral magnetic order parameter vanishes in magnitude while  $q$  stays finite. No superconductivity is seen in Fig. 6. The  $s$ -wave superconducting state is suppressed by the large value of  $U$ , and the  $d$ -wave state is not seen either since  $J$  is zero.

The energy gain of the spiral spin waves is numerically very small, of the order of a hundredth of the overall condensation energy. The introduction of a Heisenberg interaction could therefore have a large influence. To investigate this issue, we introduce a small  $J = 0.1$  while keeping  $U = 5$ , and compare Fig. 6 with Fig. 7. What was a second order transition between the SSW and the normal state for  $J = 0$  has now become first order. There is also a temperature range at which the AF is “reentrant” as a function of doping, and where the AF-SSW phase boundary move toward lower temperatures and becomes first order. When increasing  $J$ , this line of phase transitions rapidly migrate towards lower doping and very soon the whole spiral spin-wave region is gone. This explains why no spiral spin wave is seen in the phase diagrams for small  $U$  and large  $J$ .

For positive  $J$  and sufficiently low densities, the antiferromagnet and the spiral spin wave must eventually disappear, leaving room for the  $s$ -wave and  $d$ -wave superconducting states which may persist the rest of the way to zero filling. The critical temperature decreases rapidly with decreasing  $J$  and we were unable to confirm this scenario numerically.

## IX. DISCUSSION

The Hubbard model serves as a simple model for high- $T_c$  superconductors. Despite its simple appearance, the

model is still poorly understood and many sophisticated techniques for studying specific features of the model have been proposed in the literature. As a guide to this realm of possibilities, it is important to have a good understanding of all possibilities that a “simple” mean-field analysis can provide. We have therefore used a generalized Hartree-Fock-Bogoliubov theory and numerical simulations to compute phase diagrams for the extended Hubbard model. All the conventional order parameters, like  $s$ - and  $d$ -wave superconductivity, charge-density waves, and Néel and spiral antiferromagnetic states, have been included in one unifying framework, making no *a priori* assumptions about the nature of the broken symmetries. We have further shown that, in mean-field theory, no new mixed phases arise at finite doping and temperature in the extended Hubbard model with positive values of  $U$  and  $J$ . In our investigation, we have seen the time-reversal symmetry-breaking superconducting phase  $s + id$  only in a narrow region with negative  $U$ . Close to this region there is also a region of mixed antiferromagnetism and  $d$ -wave superconductivity. To place our approach in a still more general context, the mean-field method has been referred to as bosonic linearization since the Hamiltonian is expressed in terms of bosonic operators and is then linearized. Alternatively odd numbers of electron operators can be used to form new operators; the method is then called fermionic linearization.<sup>37,41</sup> This leads to a different dynamical group which has not yet been studied for the model we study here.

Our method allow phase separation to occur, which it also does in certain regions. The energy differences that we find between Néel and spiral antiferromagnets is so small, that we do not want to make any strong statements about whether phase coexistence would survive a more refined analysis or not. However, the energy difference between the AF and the normal state at the first order phase boundary is substantial. A phase separation between these two states has also been suggested both from theoretical and experimental grounds.<sup>42</sup> Another thing to keep in mind is that we require the total number of electrons to be fixed, while in the high- $T_c$  materials there are large charge reservoirs surrounding the 2D planes that are perhaps better modeled by a fixed chemical potential. Under such circumstances, the phase coexistence may well be suppressed.

There have been several earlier studies of spiral spin waves for the Hubbard model exploiting slave-boson and ordinary Hartree-Fock techniques. Most of these studies have concentrated on zero temperature, and our corresponding results are consistent with those. However, we have also extended the analysis to finite temperature.

We have concentrated on a particular extension of the Hubbard model which preserves the pseudo-spin symmetry, and we have explored the phase diagrams in many parameter regimes. However, there are very few cases where we can compare our results with the ones obtained by other extensions of the Hubbard model, like nearest-neighbor Coulomb interaction and density-dependent hopping amplitudes. The application of our method to these other cases would thus be of great interest.

Another phenomenon that we have studied is how the spiral spin waves are affected by a nearest-neighbor Heisenberg term in the Hamiltonian. We have observed that the  $(1, 0)$  spiral spin-wave phase is easily destroyed upon the introduction of a positive- $J$  Heisenberg interaction. We have mostly concentrated on spin waves in the  $(1, 0)$  direction since we found that the energy differences are very insensitive to the pitch direction, at least for the pure Hubbard model. To make the study complete, other spin directions should also be studied. However, it is likely that these small energy differences are insignificant with respect to the overall crudeness of our analysis, although one might argue that their relative difference is to be taken seriously.

#### ACKNOWLEDGMENT

The authors thank the Swedish Natural Research Council (NFR) for supporting this work.

#### APPENDIX A: THE POINT GROUP $C_{4v}$

The point-group symmetry of the 2D square lattice is  $C_{4v}$ , since the lattice is invariant under  $90^\circ$  rotations around the  $z$  axes and under reflections in the lines  $v$  and  $v'$  in Fig. 8. The group elements of  $C_{4v}$  are the identity ( $I$ ),  $90^\circ$  rotations ( $C_4$ ),  $180^\circ$  rotations ( $C_4^2$ ), reflections in  $v$  ( $\sigma_v$ ) and reflections in  $v'$  ( $\sigma_{v'}$ ). This group has four 1D irreps ( $A_1, A_2, B_1, B_2$ ) and one 2D irrep  $E$ . The character table together with examples of basis functions for the different irreps are given in Table II. Our main use of the  $C_{4v}$  irreps is to distinguish between  $d$ - and  $s$ -wave superconductivity order parameters. The  $s$ -wave ordering has the full symmetry of the lattice, i.e., it belongs to the  $A_1$  representation. The  $d$ -wave ordering, on the other hand, is antisymmetric under reflections in  $v'$ , and belongs to the  $B_1$  representation. If we would see any  $p$ -wave states, these would belong to the 2D  $E$  representation since these states are antisymmetric under parity  $[(x, y) \rightarrow (-x, -y)]$ .

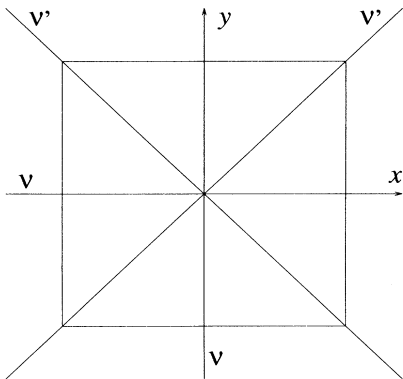


FIG. 8. The symmetry axes  $v$  and  $v'$  of the square lattice.

TABLE II. The character table of the point group  $C_{4v}$  together with examples of basis functions for the different irreducible representations.

	$I$	$C_4^2$	$C_4$	$\sigma_v$	$\sigma_{v'}$	Examples of functions
$A_1$	1	1	1	1	1	$1, \cos k_x + \cos k_y$
$A_2$	1	1	1	-1	-1	$\sin 2k_x \sin k_y - \sin 2k_y \sin k_x$
$B_1$	1	1	-1	1	-1	$\cos k_x - \cos k_y$
$B_2$	1	1	-1	-1	1	$\sin k_x \sin k_y$
$E$	2	-2	0	0	0	$\{\sin k_x, \sin k_y\}$

#### APPENDIX B: PROOFS OF THE ZERO-TEMPERATURE, HALF-FILLING THEOREMS

In this appendix we give the proofs of the theorems concerning the minimization of the ground-state energy. A bunch of related theorems have also been derived by Bach *et al.*<sup>43</sup> First we prove the lemma for how the energy minimization problem can be recast into the problem of minimizing the expectation value of the Hamiltonian written in terms of  $\langle \alpha_{\mathbf{k}}^m \rangle$ .

**Lemma 1.** *The restrictions on the expectation values  $\langle \alpha_{\mathbf{k}}^m \rangle$  for the variational solutions of Eq. (20) are  $\sum_m \langle \alpha_{\mathbf{k}}^m \rangle^2 = \frac{1}{2}$ ,  $\langle (\alpha_{00}^0)_{\mathbf{k}} \rangle = -\frac{1}{2}$ , and  $A_{\mathbf{k}} = 0 \forall \mathbf{k}$ .*

*Proof.* The space of all possible variational solutions is defined by the constraint that the Hermitian matrix  $\langle G | \Psi_{\mathbf{k}}^\dagger \otimes \Psi_{\mathbf{k}} | G \rangle$  has the four-fold degenerate eigenvalues 0 and 1, since it has the same eigenvalues as  $g = \langle G | (\chi_{\mathbf{k}}^\dagger \otimes \chi_{\mathbf{k}}) | G \rangle$ . Our aim is to find the corresponding constraints on the coefficients  $\langle \alpha_{\mathbf{k}}^m \rangle$  in the expansion

$$\langle G | \Psi_{\mathbf{k}}^\dagger \otimes \Psi_{\mathbf{k}} | G \rangle = \sum_m \langle \alpha_{\mathbf{k}}^m \rangle B_m. \quad (\text{B1})$$

First of all, since  $B_0 \equiv B_{00}^0 = -\mathbf{1}$  is the only basis matrix with a nonzero trace, one has  $\langle (\alpha_{00}^0)_{\mathbf{k}} \rangle = -\frac{1}{2}$ . Let us next define the traceless matrix  $X_{\mathbf{k}}$ ,

$$X_{\mathbf{k}} \equiv \langle G | \Psi_{\mathbf{k}}^\dagger \otimes \Psi_{\mathbf{k}} | G \rangle - \frac{1}{2} \mathbf{1}. \quad (\text{B2})$$

This matrix has the fourfold degenerate eigenvalues  $\pm \frac{1}{2}$  and the expansion

$$X_{\mathbf{k}} = \sum_{m \neq 0} \langle \alpha_{\mathbf{k}}^m \rangle B_m. \quad (\text{B3})$$

Furthermore,  $\{X_{\mathbf{k}}, X_{\mathbf{k}}\}$  has the eightfold degenerate eigenvalue  $\frac{1}{2}$ , meaning that  $\{X_{\mathbf{k}}, X_{\mathbf{k}}\} = \frac{1}{2} \mathbf{1}$ , so that using Eq. (10) we have

$$\frac{1}{2} \mathbf{1} = \{X_{\mathbf{k}}, X_{\mathbf{k}}\} = \sum_{m \neq 0} 2 \langle \alpha_{\mathbf{k}}^m \rangle^2 \mathbf{1} + A_{\mathbf{k}}, \quad (\text{B4})$$

where  $A_{\mathbf{k}}$  is the nondiagonal part defined in Eq. (37).

Since  $A_{\mathbf{k}}$  is orthogonal to  $\mathbf{1}$ , it follows that  $A_{\mathbf{k}} = 0$  and that

$$\sum_m \langle \alpha_{\mathbf{k}}^m \rangle^2 = \langle \alpha_{\mathbf{k}}^0 \rangle^2 + \sum_{m \neq 0} \langle \alpha_{\mathbf{k}}^m \rangle^2 = (-\frac{1}{2})^2 + \frac{1}{4} = \frac{1}{2}. \quad (\text{B5})$$

Q. E. D.

For some specific solutions, this lemma leads to the following theorem which considerably simplifies the search for solutions. Here we consider the larger space of solutions that arises if we disregard all constraints except the normalization  $\sum_m \langle \alpha_{\mathbf{k}}^m \rangle^2 = \frac{1}{2}$ . A solution of the new problem that happens to fulfill *all* the constraints, must then be a solution of the original problem as well.

**Theorem 1.** *Consider the Hamiltonian in Eq. (20) with fixed coefficients  $a_{l,m}$  and  $b_{l,m}$ . Define  $\mathcal{N}$  as the subset of purely quadratic and irreducible terms,  $\mathcal{N} = \{m : a_{l,m} = 0 \forall l, b_{l,m} = b_m \delta_{l,l(m)}\}$ , where  $l(m)$  is a function which attaches one single  $l$  to each  $m$ . Assume there exists an  $\tilde{m} \in \mathcal{N}$ , such that  $(b_{\tilde{m}} < 0$  and  $b_{\tilde{m}} |\beta_{\mathbf{k}}^{l(\tilde{m})} \beta_{\mathbf{k}'}^{l(\tilde{m})}| < b_m |\beta_{\mathbf{k}}^{l(m)} \beta_{\mathbf{k}'}^{l(m)}| \forall \mathbf{k}, \mathbf{k}', \forall m \in \mathcal{N} \setminus \{\tilde{m}\}$ ). If  $\langle \alpha_{\mathbf{k}}^m \rangle = 0 \forall \mathbf{k}, \forall m \in \mathcal{N} \setminus \{\tilde{m}\}$  is a sufficient condition for  $(A_{\mathbf{k}} = 0 \forall \mathbf{k})$ , then the same  $\langle \alpha \rangle$ 's will be zero also in the minimizing solution of the constrained problem.*

*Proof.* The lowest-energy solution should be minimal under any variation of  $\langle \alpha \rangle$ 's that fulfills the normalization constraint (B5). Since there is only one constraint per  $\mathbf{k}$  in the simplified problem, it is possible to keep all  $\langle \alpha \rangle$ 's fixed except two and still fulfill the constraint. Suppose that we vary only  $\langle \alpha_{\mathbf{k}}^{\tilde{m}} \rangle$  and  $\langle \alpha_{\mathbf{k}}^n \rangle$ , where  $\tilde{m}, n \in \mathcal{N}$ . A

variation around a minimizing solution must then fulfill

$$\begin{aligned} \sum_{\mathbf{k}'}'' b_{\tilde{m}} \beta_{\mathbf{k}'}^{l(\tilde{m})} \beta_{\mathbf{k}}^{l(\tilde{m})} \langle \alpha_{\mathbf{k}'}^{\tilde{m}} \rangle \delta \langle \alpha_{\mathbf{k}}^{\tilde{m}} \rangle \\ + b_n \beta_{\mathbf{k}'}^{l(n)} \beta_{\mathbf{k}}^{l(n)} \langle \alpha_{\mathbf{k}'}^n \rangle \delta \langle \alpha_{\mathbf{k}}^n \rangle = 0, \\ \langle \alpha_{\mathbf{k}}^{\tilde{m}} \rangle \delta \langle \alpha_{\mathbf{k}}^{\tilde{m}} \rangle + \langle \alpha_{\mathbf{k}}^n \rangle \delta \langle \alpha_{\mathbf{k}}^n \rangle = 0. \quad (\text{B6}) \end{aligned}$$

From our assumptions, we have  $b_{\tilde{m}} < 0$ , and to consider competing solutions one must also have  $b_n < 0$ . Since there are no constraints imposed on the signs of  $\langle \alpha_{\mathbf{k}}^{\tilde{m}} \rangle$  and  $\langle \alpha_{\mathbf{k}}^n \rangle$ , it is obvious that a minimizing solution is obtained by choosing  $\text{sgn}(\langle \alpha_{\mathbf{k}}^{\tilde{m}} \rangle) = \text{sgn}(\beta_{\mathbf{k}}^{l(\tilde{m})})$  and similarly for  $\langle \alpha_{\mathbf{k}}^n \rangle$ . Taking these sign considerations into account and eliminating  $\delta \langle \alpha_{\mathbf{k}}^{\tilde{m}} \rangle$  and  $\delta \langle \alpha_{\mathbf{k}}^n \rangle$  yields

$$\begin{aligned} \sum_{l, \mathbf{k}'}'' (b_{\tilde{m}} |\beta_{\mathbf{k}}^{l(\tilde{m})} \beta_{\mathbf{k}'}^{l(\tilde{m})}| |\langle \alpha_{\mathbf{k}'}^{\tilde{m}} \rangle \langle \alpha_{\mathbf{k}}^n \rangle| \\ - b_n |\beta_{\mathbf{k}}^{l(n)} \beta_{\mathbf{k}'}^{l(n)}| |\langle \alpha_{\mathbf{k}'}^n \rangle \langle \alpha_{\mathbf{k}}^{\tilde{m}} \rangle|) = 0. \quad (\text{B7}) \end{aligned}$$

Summing this equation over  $\mathbf{k}$  gives

$$\sum_{\mathbf{k}, \mathbf{k}'}'' (b_{\tilde{m}} |\beta_{\mathbf{k}}^{l(\tilde{m})} \beta_{\mathbf{k}'}^{l(\tilde{m})}| - b_n |\beta_{\mathbf{k}}^{l(n)} \beta_{\mathbf{k}'}^{l(n)}|) |\alpha_{\mathbf{k}}^{\tilde{m}} \alpha_{\mathbf{k}}^n| = 0, \quad (\text{B8})$$

and since from our assumption,  $b_{\tilde{m}} |\beta_{\mathbf{k}}^{l(\tilde{m})} \beta_{\mathbf{k}'}^{l(\tilde{m})}| < b_n |\beta_{\mathbf{k}}^{l(n)} \beta_{\mathbf{k}'}^{l(n)}| \forall \mathbf{k}, \mathbf{k}'$ , the solution must be either  $\alpha_{\mathbf{k}}^{\tilde{m}} = 0 \forall \mathbf{k}$  or  $\alpha_{\mathbf{k}}^n = 0 \forall \mathbf{k}$ . Of these two,  $\alpha_{\mathbf{k}}^n = 0$  is obviously the solution of lowest energy. This argument is then applied to all purely quadratic terms  $n \in \mathcal{N} \setminus \{\tilde{m}\}$ .

Q. E. D.

- \* Present address: Nordita, Blegdamsvej 17, DK-2100 København Ø, Denmark.
- <sup>1</sup> C. N. Yang and S. C. Zhang, *Mod. Phys. Lett. B* **4**, 759 (1990).
  - <sup>2</sup> B. L. Shraiman and E. D. Siggia, *Phys. Rev. Lett.* **62**, 1564 (1989).
  - <sup>3</sup> H. J. Schulz, *Phys. Rev. Lett.* **64**, 1445 (1990).
  - <sup>4</sup> E. Arrigoni and G. C. Strinati, *Phys. Rev. B* **44**, 7455 (1991).
  - <sup>5</sup> M. Dzierzawa, *Z. Phys. B* **86**, 49 (1992).
  - <sup>6</sup> S. Sarker, C. Jayaprakash, H. R. Krishnamurthy, and W. Wenzel, *Phys. Rev. B* **43**, 8775 (1991).
  - <sup>7</sup> R. Micnas, J. Ranninger, and S. Robaszkiewicz, *Rev. Mod. Phys.* **62**, 113 (1990).
  - <sup>8</sup> M. Ozaki, *Int. J. Quantum Chem.* **42**, 55 (1992).
  - <sup>9</sup> M. Ozaki and H. Kohno, *Prog. Theor. Phys.* **84**, 1053 (1990).
  - <sup>10</sup> R. Micnas, J. Ranninger, S. Robaszkiewicz, and S. Tabor, *Phys. Rev. B* **37**, 9410 (1988).
  - <sup>11</sup> R. Micnas, J. Ranninger, and S. Robaszkiewicz, *J. Phys. C* **21**, L145 (1988).
  - <sup>12</sup> R. Micnas, J. Ranninger, and S. Robaszkiewicz, *Phys. Rev. B* **39**, 11 653 (1989).
  - <sup>13</sup> B. R. Bulka, *Physica C* **165**, 449 (1990); *Physica B* **165**, 1037 (1990); *Phys. Status Solidi B* **163**, 193 (1991).

- <sup>14</sup> J. L. Birman and A. I. Solomon, in *Dynamical Groups and Spectrum Generating Algebras*, edited by A. Bohm, Y. Ne'eman, and A. O. Barut (World Scientific, Singapore, 1988).
- <sup>15</sup> N. N. Bogoliubov, *Sov. Phys. JETP* **7**, 41 (1958); *Nuovo Cimento* **7**, 794 (1958).
- <sup>16</sup> J. G. Valatin, *Nuovo Cimento* **7**, 843 (1958).
- <sup>17</sup> R. Balian and N. R. Werthamer, *Phys. Rev.* **131**, 1553 (1963).
- <sup>18</sup> M. Ozaki, *J. Math. Phys.* **26**, 1514 (1985).
- <sup>19</sup> A. I. Solomon and J. L. Birman, *Phys. Lett. A* **104**, 235 (1984); *J. Math. Phys.* **28**, 1526 (1987); *J. Phys. C* **21**, L751 (1988).
- <sup>20</sup> R. H. McKenzie and J. A. Sauls, *Helium Three (Modern Problems in Condensed Matter Sciences)* (Elsevier Science, Amsterdam, 1990), p. 225.
- <sup>21</sup> W. Metzner and D. Vollhardt, *Phys. Rev. B* **39**, 4462 (1989).
- <sup>22</sup> A. Schadschneider, *Phys. Rev. B* **51**, 10 386 (1995).
- <sup>23</sup> J. de Boer, V. E. Korepin, and A. Schadschneider, *Phys. Rev. Lett.* **74**, 789 (1995).
- <sup>24</sup> F. H. L. Eßler, V. E. Korepin, and K. Schoutens, *Phys. Rev. Lett.* **68**, 2960 (1992); **70**, 73 (1993).
- <sup>25</sup> A. Montorsi and M. Rasetti, *Phys. Rev. Lett.* **66**, 1383 (1991).

- <sup>26</sup> S. C. Zhang, Phys. Rev. Lett. **65**, 120 (1990).
- <sup>27</sup> S. C. Zhang, Int. J. Mod. Phys. B **5**, 153 (1991).
- <sup>28</sup> S. C. Zhang, Phys. Rev. B **42**, 1012 (1990).
- <sup>29</sup> S. Östlund and G. Mele, Phys. Rev. B **44**, 12 413 (1991).
- <sup>30</sup> S. Östlund, Phys. Rev. Lett. **69**, 1695 (1992).
- <sup>31</sup> J. B. Marston and I. Affleck, Phys. Rev. B **39**, 11 538 (1989).
- <sup>32</sup> H. Shiba, Prog. Theor. Phys. **48**, 2171 (1972); V. J. Emery, Phys. Rev. B **14**, 2989 (1976).
- <sup>33</sup> E. Fradkin, *Field Theories of Condensed Matter Systems* (Addison-Wesley, Redwood City, CA, 1991).
- <sup>34</sup> E. H. Lieb and F. Y. Wu, Phys. Rev. Lett. **20**, 1445 (1968).
- <sup>35</sup> W. Miller, Jr., *Symmetry Groups and their Applications* (Academic, New York, 1972).
- <sup>36</sup> See, for example, J. W. Negele and H. Orland, *Quantum Many-Particle Systems* (Addison-Wesley, Redwood City, CA, 1988).
- <sup>37</sup> A. Montorsi, M. Rasetti, and A. I. Solomon, Phys. Rev. Lett. **59**, 2243 (1987).
- <sup>38</sup> We observe that the states in the corollary are exactly the states termed “unitary states” by A. I. Solomon and J. L. Birman, Phys. Lett. A **111**, 423 (1985).
- <sup>39</sup> W. H. Press, S. A. Teukolsky, W. T. Vetterling, and B. P. Flannery, *Numerical Recipes in Fortran*, 2nd ed. (Cambridge University Press, Cambridge, England, 1992).
- <sup>40</sup> R. Strack and D. Vollhardt, Phys. Rev. Lett. **72**, 3425 (1994).
- <sup>41</sup> A. Danani, M. Rasetti, and A. I. Solomon, in *Theories of Matter*, edited by A. Solomon (World Scientific, Singapore, 1994).
- <sup>42</sup> V. J. Emery and S. A. Kivelson, Physica C **209**, 597 (1993), and references therein.
- <sup>43</sup> V. Bach, E. H. Lieb, and J. P. Solovej, J. Stat. Phys. **76**, 3 (1994).

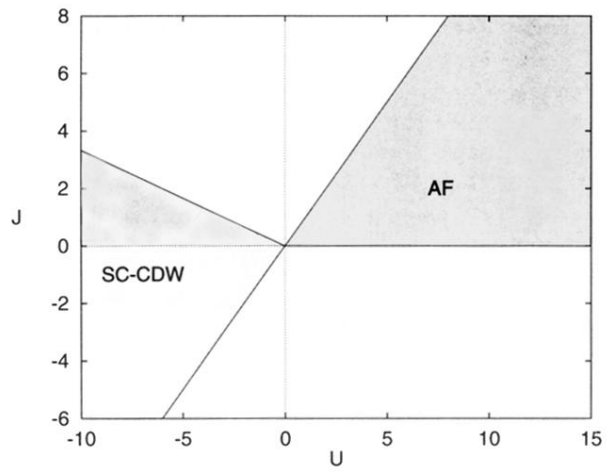


FIG. 2. The low energy states of the extended Hubbard model according to Corollary 1 is shown in grey. The white areas are indeterminate from the corollary, and the phases here must be computed numerically.